Diamond & Related Materials 150 (2024) 111746

Contents lists available at ScienceDirect

Diamond & Related Materials

journal homepage: www.elsevier.com/locate/diamond

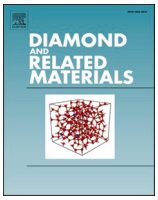

Fe_3O_4 nanoparticles decorated on N-doped graphene oxide nanosheets for elimination of heavy metals from industrial wastewater and desulfurization

Kashinath Lellala [a,*], Subhendu Kumar Behera [b], Prarthana Srivastava [c], Waseem Sharaf Saeed [d], Ahmed S. Haidyrah [e], Ajay N. Burile [f,*]

[a] Centre for Materials Science and Technology, University of Mysore, Mysore 570005, India
[b] Electronics & Telecommunication Engineering, DRIEMS University, Tangi, Cuttack, 754 022, Odisha, India
[c] Department of applied sciences, KIET group of institutions, Delhi NCR, Ghaziabad 201206, India
[d] Department of Restorative Dental Sciences, College of Dentistry, King Saud University, P.O. Box 60169, Riyadh 11545, Saudi Arabia
[e] Strategy & Institutional Excellent Sector, King Abdulaziz City for Science and Technology (KACST), Riyadh 11442, Saudi Arabia
[f] Priyadarshini Bhagwati College of Engineering, Harpur Nagar, Umred Road, Nagpur, 440024, Maharashtra, India

ARTICLE INFO

Keywords:
Heavy metals
Iron oxide
Desulfurization
Sulfur
Graphene oxide
Adsorption and microwave treatment

ABSTRACT

Finding an effective and excellent pertinent single catalyst material for multipurpose application for the purification of hydrocarbons in fuels (desulfurization), and for efficient removal of heavy metals from industrial effluent is greatly endowed. In the present work, a hybrid nanocomposite of ultrafine magnetite (Fe_3O_4) nanoparticle embedded on the surface of *in-situ* nitrogen doped layered GO (NGO) sheets were fabricated by sol-gel method and treatment with microwave irradiation technique is reported for the first time. The results show a high removal efficiency of 97 % for multiple heavy metals (Pb^{2+}, Cd^{2+}, Cu^{2+}, Cr^{+2}, Mn^{+2} *etc.*) in industrial effluent and as well as in synthetic water with a very good retention performance of 99 %. The composites were tested against the elimination of sulfur from thiophene is 1.495 mmol g^{-1} is reported high is due to coupling and coordination of nitrogen with Fe—O and C. Recycling studies showed that the developed composites had excellent recyclability, with <82 % removal at the 5th cycle; its feasibility was evaluated using industrial effluent water and in synthetic water. Surface phenomena studies presented here revealed that the adsorptive removal processes of heavy metals involved π electron donor-acceptor interactions, ion exchange, and electrostatic interactions, along with surface complexation that showed an excellent synergism. A high stability, and retention performance is better than the pure Fe_3O_4 and NGO sheets. We hope that this study will motivate and give further scope for scientists working on magnetite-based graphene nanocomposites.

1. Introduction

The environment is highly adulterated with the presence of heavy metals which is a major concern and there is an alarming need to protect and safeguard the human being and environment. The heavy metals and their contaminations will not degrade easily like the organic pollutants in wastewater [1,2]. Thus, elimination of heavy metal toxicity from water and effluents needs a keen interest for the concentrations of metals into smaller volume charted by recovery or for any safe disposal [3,4]. Yin et al., (2012) reported various magnetic materials used to show the high potential adsorption of metals from wastewater, including magnetic adsorbents ranging from micro to nano scale [5]. Xue *et al* (2011). reported the magnetic nanoparticles anchored to GO (GO)/reduced GO (rGO) sheets which allows higher loading efficiency and homogenous distribution giving rise to magnetic nanocomposites for the potential applications [6]. The predominant availability of functional groups and interaction of π stacking on the surface of GO nanosheets makes the materials very active for the removal of heavy metals and necessary potential for adsorption capacity [7,8]. Yang *et al* (2014) reported 92.65 mg/g chromium adsorption at favourable *pH* conditions [9,10]. Guo *et al* (2014) showed an adsorption capacity of 17.29 mg/g using functionalized graphene with ferro/ferric oxide composites for removal of chromate ion [11,12]. Zhu *et al* (2011) synthesized the core-shell graphene Fe–Fe2O3 nanoparticles which showed efficient adsorption capacity for As (III) in polluted water. The use of GO as active adsorbent for rapid removal of ionic species such as lead, cadmium, cobalt, and other

* Corresponding authors.
E-mail addresses: kashinathlellala@gmail.com (K. Lellala), ajayburilepbcoe@gmail.com (A.N. Burile).

https://doi.org/10.1016/j.diamond.2024.111746
Received 8 August 2024; Received in revised form 15 October 2024; Accepted 3 November 2024
Available online 6 November 2024

adsorption/sorption application is well organized [13,14]. Recently, Lingamdinne et al. employed porous inverse spinel composite (MGO) and porous inverse rMGO nanocomposites using nickel ferrite and GO, and applied them for the removal of arsenic chromium and lead. The qmax for MGO and rMGO was (82.47 and 121.95 mg/g) for Pb (II), and (87.49 and 126.58 mg/g) for Cr(III), respectively, and could be regenerated and reused up to 5 cycles, without any significant loss in their removal efficiency (Lingamdinne et al., 2016b, 2017b, 2018). Liu et al. prepared FeS/MXene nanocomposite using the self-assembled method to decontaminate Cr(*VI*)ions from aquatic environments showed exceptional adsorption capacity (107.2 mg/g) for Cr(*VI*)ions at pH 1 [53]. Furthermore, the As@GO membrane also demonstrates excellent rejection of up to 95.6 % and 96.7 % for cadmium (Cd2+) and lead (Pb2+) ions, respectively. L.P. Lingamdinne et al. reported the removal of Pb2+ and Cr3+ using rGO-Mn3O4 composites achieving maximum sequestration capacities of 130.28 and 138.51 mg g−1 for Pb2+and Cr3+, respectively, according to the Langmuir mode [45–49]. Inamullah Mahar reported the fabrication and characterization of MXene/carbon composite-based nanofibers (MXene/CNFs) membrane: An efficient adsorbent material for removal of Pb + 2 and As+3 ions from water showed high adsorption capability for Pb2+ (12.5 mg.g-1) and As3+ (3.3 mg.g-1) at an optimized neutral pH within 20 and 30 min respectively [53]. The removal rates for Pb2+ and As3+ ions were achieved at 89 % and 81 % respectively which are much sufficient to treat contaminated water at low concentrations (10 μgL-1 to 10 mgL-1). Recently Kashinath L reported the synthesis of sulfur embedded on *in-situ* carbon nano-disc decorated on graphene sheets for efficient photocatalytic activity and capacitive deionization method for heavy metal removal efficiency of 90 % [50]. Hyder Ali reported the synthesis of MXene-based nanocomposites: emerging candidates for the removal of antibiotics, dyes, and heavy metal ions from wastewater with removal efficiency of 87 % [52]. S. Charazińsk reported the efficiency of removing heavy metal ions from industrial electropolishing wastewater containing high concentrations of metal ions Fe(III), Cr(III), Ni(II), and Cu(II) using natural materials [57]. Ashique Hussain Jatoi reported the fabrication of High-performance asparagine-modified graphene oxide membranes for organic dyes and heavy metal ion separation with an exceptional water permeability ofB1740 10 L m2h1bar1 [58] (Table 1).

Another important environmental issue is purification of liquid fuels (hydrocarbons) for energy sources, fuel cells, and electrical generators, *etc.* Thus, the purification of fuels are now-a-days are drawing great attention due to the rules and regulations of environmental and fuel cells applications. Amongst, sulfur compounds are poisonous having negative impacts on human health and dreadful to electrochemical/catalytic materials in fuel cells [15,16]. Removal of sulfur was carried out by hydro-desulfurization (HDS) conducted at high temperatures and in high pressures was in practice but targeting the materials at high temperature and pressure was a very difficult task. The researchers are motivated to use non-HDS materials as a promising adsorption candidate because of its cost-effective and feasibility in favourable conditions [17–19]. Besides, materials with higher surface area and mesoporous structure have been employed as functional adsorbents for the removal of sulfur compounds like mesoporous silica, alumina, zeolite, metal–organic frameworks and activated carbon. The removal of sulfur using CuCl supported by activated carbon is 1.748 mg/g and Fe_3O_4@C reported value is 0.483 mg/g at 140 *ppmw* from thiophene [19,20]. Peng Tan et al. reported the core shell synthesis of AgNO3/Fe3O4@mSiO for sulfur capture from thiophene. The regenerated adsorbent after six cycles still shows a good adsorption capacity (0.145 mmol g-1 or 4.64 mg/g), which is comparable to the fresh adsorbent (0.147 mmol g-1 or 4.70 mg/g) [56]. From the above discussions and literature data of the magnetite-graphene (Fe_3O_4-GO) based composites have been used for many potential applications, but the selection of efficient and potential adsorption materials for the multi-functional purpose is very hard and difficult to find [21–23] and the efficiency/stability of the materials are decaying during the long run application. However, there is still a scope for developing non-precious hybrid nanocomposites with excellent properties for multi-functional applications. Recently, researchers are using nitrogen-doped GO (NGO) materials for many potential applications like a supercapacitor, energy storages, fuel cells, and as adsorption/ capacitive materials. The nitrogen doping can effectively suppress and prevent the aggregation or restacking of graphene sheets and additionally, it can facilitate in providing a lone pair of electrons that increases the electron density of graphene, in turn, generates higher current density and surplus increase in electrical conductivity [24]. Besides, NGO offers more active sites for the nucleation, which facilitates the control of morphology and particle size of hybrid materials and strengthen the interaction. NGO acts as a matrix for host materials which supportively increases the performance and exhibits excellent synergetic effect [25,26]. NGO can facilitate a porous structure and exhibits a higher stability of absorptions and excess of electron density can be used for adsorption/sorption [27]. In the present work, sol-gel aided microwave synthesis method is employed to fabricate a highly efficient adsorptive/sorption materials. Herein, ultrafine magnetite nanoparticles were decorated on the active sites of nitrogen-doped GO nanosheets has been reported [8,28,29]. The coupling of magnetite nanoparticles and nitrogen doped GO approach is being selectively used for multi-functional applications, which will enhance the performance of adsorptive study for rapid removal of heavy metal from wastewater, industrial effluent and desulfurization is reported to be a newest. This new insight coupling method and materials approach can be used for the fabrication of advanced functional materials for many potential applications as multifunctional materials with excellent performance and it will open a new futuristic venue for researchers [30].

Table 1
Shows the heavy metal removal efficiency of Fe_3O_4-NGO compared with other nanomaterials.

Adsorbent	Method	Removal of heavy metals	Ref
Fe_3O_4-NGO	Sol-gel assisted microwave method	Pb 190.00, Cr 160, Cd 67, Cu 95, Zn 100, Ni 85 mg. g^{-1}	This study
rGO-Mn3O4	Hydrothermal	Pb2+ 130.28 mg g − Cr3 + 138.51 mg g − 1	[45]
MXene/carbon composite	Chemical synthesis	Pb2+ (12.5 mg.g-1) and As3+ (3.3 mg.g-1)	[52]
As@GO membrane	Chemical synthesis	lead (Pb2+) 95.6 % and 96.7 % for cadmium (Cd2+)	[54]
MnO2/MXene	Hydrothermal method	Pb(II) 0.001235 206	[50]
FeS/MXene	Self-assemble method	Cr(VI) 107.2	[53]
Magnetic graphene oxide	Hydrothermal and chemical method	Pb 200.00, Cr 24.1, Cu 62.89, Zn 63.69, Ni 51.02 mg.g^{-1}	[57]

2. Experimental methodology

2.1. Materials

The chemicals and reagents used in the sorption studies are of analytical grade. Ferric chloride hexahydrate, potassium permanganate, sodium hydroxide, ammonia and hydrogen peroxide, lead nitrate, chromium nitrate and cadmium nitrate were procured from Sigma Aldrich, India and Graphite powder (MERCK, India). Concentrated hydrochloric acid and sulphuric acid of 98 % purity were also procured from Sigma Aldrich, India. The industrial effluent was collected from the industrial area, Mysore, India, containing maximum heavy metals like Cu, Pb, Cd, Co, Zn, Mn, Al, and Ni. For the preparation of simulated/ synthetic heavy water, 0.01 M of respective nitrate (lead, cadmium and chromium) is mixed with 1000 mL of distilled water individually.

2.2. Synthesis of GO sheets

2 g of graphite and 1 g of sodium nitrate was dissolved in 60 mL of pre-cooled sulphuric acid and was allowed to stir for 45 min in ice cool bath conditions. After that, 6 g of $KMnO_4$ was added slowly with constant stirring and then 280 mL of deionized water was added to it which was again subjected to continuous stirring for 1 h to obtain the homogeneous solution. To this solution 10 mL of hydrogen peroxide was added and stirred for almost 30 min. Then the solution was thoroughly washed and filtered with the dilute HCl solution (2/20) volume by volume prepared in distilled water. The product was recovered from centrifugation and dried at 80 °C in vacuum condition for 24 h. The product so obtained is a fine powder of GO nanosheets [30,31].

2.3. Preparation of hybrid nanocomposites

5 mmol of $FeCl_3.6H_2O$ and 0.1 mmol of NaOH each was prepared in 20 mL deionized water and was further added in dropwise to GO solution (a homogeneous solution of GO was prepared by adding 0.2 g of the above prepared GO nanosheets in 100 mL of deionized water followed by sonicating for 45 min for future exfoliation) with constant stirring at 80 °C [32]. Then 10 mL of $NH_3H_2O_2$ solution was prepared by adding 40 mL of deionized water which was further added dropwise slowly to the complex solution at 80 °C and was subjected to stirring for 1 h until a stable viscous suspension is obtained. The complex solution was exposed to microwave irradiation for 10 min at 900 W and washed several times with deionized water. Then the resultant adsorbent underwent centrifugation at 5000 rpm. The adsorbent so obtained was vacuum dried at 80 °C for 24 h to harvest powdered magnetite-nitrogenous graphene nanocomposites are named as 1@Fe-NGO. The same procedure was adopted for the synthesis 0.5@Fe-NGO (2.5 mmoles, $FeCl_3.6H_2O$) and 0.25@Fe-NGO (1.25 mmole, $FeCl_3.6H_2O$) respectively. The nitrogen doped graphene oxide was synthesized in similar procedure in the absence of $FeCl_3.6H_2O$ and pure Fe_3O_4 nanoparticles were synthesized under similar conditions in the absence of GO and NH_3H_2O.

2.4. Characterizations

The crystallographic structure of the synthesized materials were studied using Rigaku Smart Lab–II, CuKα radiation (λ = 1.544 Å) 40 KeV and 30 mA. Fourier transformed infrared spectroscopy (FTIR) (Jasco FTIR-460) plus spectrophotometer was used to determine the functional groups. The absorption diffused reflectance spectra were studied using a Diode Array single beam Spectrometer (SA-165), ELICO, India. Nitrogen adsorption/desorption and surface area measurements analysis was performed at 77 K using a BELSORP Mini-II system, Japan. The binding energy was investigated by the X-ray Photoelectron Spectrometer technique (ULVAC-PHI). The microstructural behavior of the composites was observed using a scanning electron microscope (Carl Zeiss, Sigma 500). The electrons were accelerated at the rate of 5 kV voltage. The higher the accelerating voltage, the greater will be the penetrating power of beam into the samples. The identification of size, shape and microstructural analysis requires a high-resolution transmission electron microscope which was carried using (Jeol JEM-2100).

2.5. Adsorption experiments (synthetic water and industrial effluent water)

The materials synthesized were studied for adsorption experiments against the removal of heavy metals present in the industrial effluent and in simulated water with different *pH* variations at the ambient room temperature. The carcinogenic heavy metals like cadmium, lead, and chromium were detected and the adsorption percentage was calculated to find the kinetics and mechanism of the catalytic processes. In the experimental studies, 10 mg of the adsorbent Fe_3O_4-NGO (10 mg/mL Fe_3O_4-NGO aqueous dispersion) was dispersed in 100 mL of industrial effluent and simulated water containing heavy metals. After adsorption experiments, the solution was centrifuged at 10000 rpm in order to separate the supernatant for determination of removal efficiency. The concentration of heavy metal ions in the solution after adsorption was examined by inductively coupled plasma mass spectrometry (ICPMS) at regular interval of 30 mins. The amount of heavy metal ion adsorbed on the adsorbent at the time interval of 30 mins [33,34] q_t was determined from the given equation

$$q_t = (C_o/C_e) \tag{1}$$

Where C_o and C_e - initial and equilibrium concentration (mg/L) of metal ion, V is the volume of solution (mL), and m is the weight of Fe_3O_4-GO in g. Additionally, adsorptions studies were carried out in batch methods dissolving 0 to 600 *ppmw* (parts per million weights) of sulfur content in thiophene. The adsorption studies were carried out by adding 5 mg of catalyst to the fuel and was subjected to 3 h of constant shaking. The sulfur content treated with prepared materials were identified using flame photometric detector attached with Varian 3800 Gas Chromatograph (GC).

2.5.1. Adsorption kinetics and isotherms

The Kinetic studies were conducted by varying the initial concentration of the metal ions of Pb (II), Cd (II), Co (II), Zn (II), and Ni (II) respectively. The adsorbate mixture was taken in 500 mL conical flask that was placed in a thermostatically controlled water bath at 25 °C with constant stirring. 10 mg of the synthesized composites (Fe_3O_4_NGO) was added to the flask. Throughout the adsorption experiments, small fractions of the sample were taken out for analysis at a predetermined interval and then were centrifuged for 10 min to separate the supernatant and the adsorbent. The final metal ion concentration of the supernatant obtained was determined by ICPMS at different time intervals. The rate expressions for pseudo-first order and pseudo second order kinetic model is expressed as follows [35,36] where k_1(1/min) and k_2 (L /mol min) is the adsorption rate constants corresponding to the first and second order kinetic models, respectively, q_t (mg/g) and q_e (mg/g) represents the amount of adsorbate adsorbed at equilibrium and at time t respectively.

2.5.2. Thermodynamics

A thermodynamic study offers insights into the minimum kinetic energy necessary for the adsorbate to become bound to the adsorption site and can be evaluated as endothermic/exothermic reaction mechanism using the thermodynamic parameters such as such as the Gibbs free energy change (ΔG °, kJ/mol), the standard enthalpy change (ΔH°, kJ/mol), and the standard entropy change (ΔS°, J/mol K^{-1}) [61]. These parameters can be calculated by the following equations stated as (Eqs. (2)–(5)):

$$\Delta G^{\circ} = -RTlnkc \tag{2}$$

$$lnKc = Cad, eCe \tag{3}$$

$$lnKc = -\Delta H0RT + \Delta S0R \tag{4}$$

$$\Delta G^{\circ} = \Delta H^{\circ} - T\Delta S \tag{5}$$

where R represents the universal (ideal) gas constant (8.314 J/mol K), T is the temperature in Kelvin (K); Kc is the apparent equilibrium adsorption [59,60] or the Langmuir isothermal constant [61]; Cad, and eCe are the concentration (mg/L) of heavy metal in adsorbent and in solution, respectively. ΔH0 and ΔS0 values can be calculated at different temperatures, assuming these parameters to be independent of temperature. A negative or positive value ΔG° at a known temperature confirms the spontaneity (or non-spontaneity) of the adsorption process, a positive value of ΔH° suggests the endothermic nature of the adsorption of a pollutant by the sorbent, and a positive value of ΔS° illustrates

an increase in the randomness of the adsorption process [61,62]. The thermodynamic properties associated with the removal of metal ions exhibit variation due to the adsorbent's composition, structure, and surface characteristics, leading to different affinities for metal ion removal. Enhanced surface area and a porous structure can promote interactions and subsequent adsorption. Factors like the presence of competing ions and shifts in pH can modify the charge distribution on both the metal ion and adsorbent surfaces, thereby influencing thermodynamic equilibrium. Additionally, distinct metal ions possess varying thermodynamic affinities due to their unique electronic configurations and charge densities [22,94]. The spontaneous endothermic adsorption behaviours of Pb^{2+} and Cr^{3+}. Cd^{+2} were demonstrated by thermodynamic investigations. Batch tests and XPS analysis revealed that the main mechanisms for heavy metal ions removal were π electron donor-acceptor interaction, ion-exchange, electrostatic interaction, and surface complexation.

3. Results and discussion

3.1. XRD patterns

Fig. 1a shows the crystalline nature of the synthesized hybrid nanocomposites, Fe_3O_4 and NGO nanosheets respectively. The diffraction peaks patterns of Fe_3O_4-NGO nanocomposites are located at 18° (111), 30.5°(220), 35.7°(311), 37.5°(222), 46.7°(400), 58.5°(511), and 70.1°(444) respectively. These reference planes are inconsistent with standard X-ray diffraction peak patterns of JCPDS No: 89-0950 of face-centred cubic crystalline plane structure of Fe_3O_4 nanoparticles spectrum. A similar diffraction pattern was observed for different molar concentrations of Fe_3O_4-NGO composites. 1@Fe-NGO (1 mol concentration of Fe_3O_4), 0.5@Fe-NGO (0.5 mol concentration of Fe_3O_4) and 0.25@Fe-NGO (0.25 mol concentration of Fe_3O_4) respectively as shown in Fig. 1a. It can be depicted from the Fig. 1a that there is a small peak at 26° which indicates the presence of graphene in the nanocomposites. This small peak confirms that the NGO has been reduced to graphene in the synthesis process. The nanocomposites are having crystalline behavior and fine structure that of magnetite nanoparticles which can investigated from the presence of major peak at 30.5°. As the molar concentration of Fe_3O_4 increases, it can be predicted that the intensity of major peak also increases which confirms the crystalline behavior and higher amount of magnetite particles participation in the composite's material. The peak at 10° diminished slowly as the Fe content increases which confirms the magnetite nature of nanoparticles [37]. The diffraction patterns of NGO are located at 10° (002) and 43° (101) respectively as shown in Fig. 1a. The presence of additional peaks at 26° and 43° indicates the reduction of GO synthesized is a layered structure formation and is due to the presence of graphene/reduced GO structure and diffraction patterns confirm the NGO is having a less functional group of hydroxyl and epoxy.

3.2. FTIR analysis

Fourier transformer infrared (FTIR) spectroscopy was employed to understand the covalent functionalization of NGO, Fe_3O_4 and hybrid nanocomposites of Fe_3O_4-NGO. The spectra of NGO, Fe_3O_4-NGO nanocomposites (0.25@Fe-NGO, 0.5@Fe-NGOand1@Fe-NGO) are shown in Fig. 1b. The absorption spectra for NGO was located at 1078 cm^{-1} (C—O, alkoxy) stretching vibration mode, 1180 cm^{-1} (C—O, epoxy), 1475 cm^{-1} (C-OH carboxyl), 1625 cm^{-1} (C=C), and 1742 cm^{-1} (C═O, carboxyl) and the peak at 2952 cm^{-1} (C—H bond) as shown in inset image of Fig. 1b. Fig. 1b depicts the spectra of Fe_3O_4 subjected peaks at 570 and 1059 cm^{-1} confirming bonding of Fe and O to form magnetite material. In contrast, the FTIR spectra of NGO and NGO/Fe_3O_4 clearly confirm that several oxygen functional groups were mostly decreased or ceased in the synthesis process. This confirms the successful reduction of NGO and in turn generates the reduced form of GO that played a vital role in increasing the surface area and higher adsorption due to nitrogenous graphene nature which is illustrated in the inset image of Fig. 1b [28]. The synthesized samples were characterized using FTIR after the performance of adsorption test is shown in supplementary Fig. S1a. From the spectra, it can be predicted that there is a widening or stretching of area around the finger print region of metal oxide which predicts a higher amount of metal incorporation or metal embedded that are due recovery of heavy metal from industrial effluent and synthetic water. Additionally, there is broadening of OH peaks which suggest a heavy metal oxidization that leads to the formation of metal-based oxides. The spectra patterns of sample after the test and before the test shows a big difference that confirms the presence of extra or heavy metal recovery and changes in the chemical absorption. When compared NGO sample showed a lower peak pattern that of Fe_3O_4-NGO sample, that directly confirms and revels the participation of iron oxide on the surface of NGO sheets. This change shows a very good retention and recovery of heavy metal by the synthesized heterostructure composites.

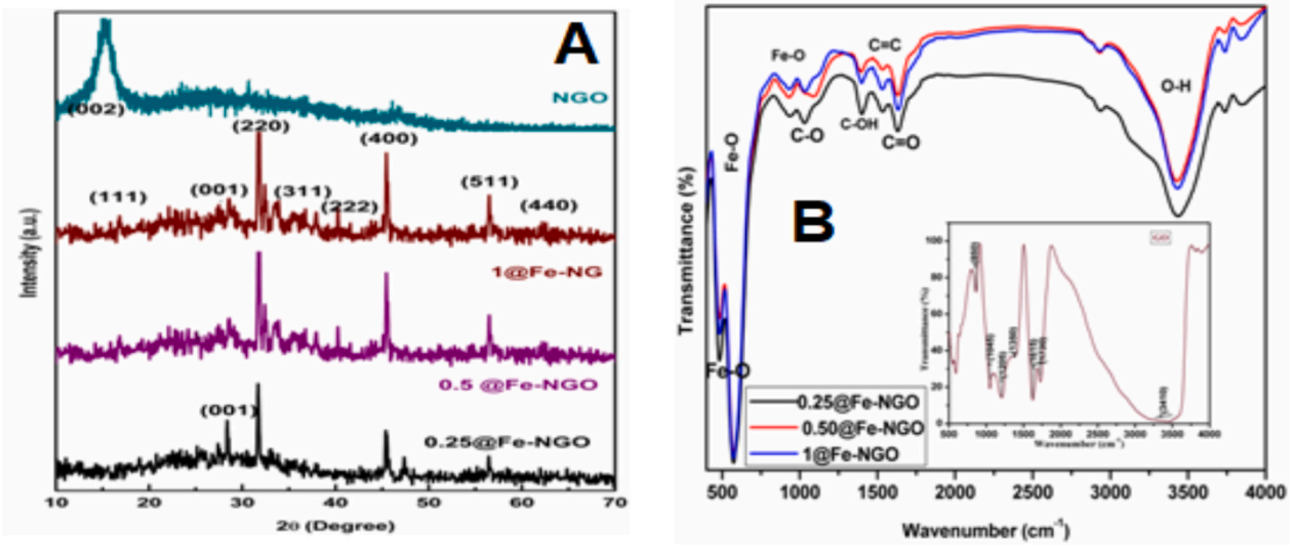

Fig. 1. a) XRD patterns; and b) FTIR spectra of 0.25@Fe-NGO, 0.5 @Fe-NGO, 1@Fe-NGO, and NGO.

3.3. Structure and morphology of the composites

The microstructural analysis of the pure Fe_3O_4, NGO sheets, and Fe_3O_4-NGO hybrid nanocomposites were explored using a scanning electron microscope (SEM) and high-resolution transmission electron microscope (HR-TEM) as shown in Fig. 2. From the images of SEM, it can be predicted that isometric/spherical like structure are confirmed for pure Fe_3O_4 as shown in Fig. 2(b) and crimpled/wrinkled paper-like sheets (layered) are observed for pure NGO as shown in Fig. 2(a). The SEM images of Fe_3O_4-NGO composites reveal the confirmation of spherical/isometric nanoparticles decorated on the surface of layered nitrogenous GO sheets for the 1@Fe-NGO respectively as shown in Fig. 2 (c). Additionally, in-depth microstructural properties of composites were studied using HR-TEM as shown in Fig. 2(d-f). The wrinkled or crushed like a porous sheet was observed for NGO (Fig. 2d) and isometric nanoparticles of Fe_3O_4 embedded on the layered surface of NGO as shown in Fig. 2(e-f) with high and low magnifications. The dark black colour sized particles are due to the presence of iron oxide on the grey coloured surface indicates NGO sheets. These images clearly shows the evidence of iron oxide nanoparticles decorated/embedded on the layered surface of *in-situ* nitrogen-doped GO sheets [38,39]. The interplanar d spacing of Fe_3O_4 and NGO can be easily identified from low magnified HR-image shown in the inset image of Fig. 2(e-f) which agrees well with the crystalline diffraction data of XRD. The structure and morphology of the sample were tested after the adsorption test using SEM technique. From the images, it is predicted that there is no much changes in the structure of the materials that confirms rigidity and robust nature of synthesized heterostructure but a few micro or nano surface and holes on the surface of NGO were covered due to extra materials embedding that are recovered heavy metals. The change in porosity and surface area measurement can identified by the BET results after the adsorption test shown in FigS1b. The decrease in surface area and porous nature of NGO is comparatively lower than the Fe_3O_4-NGO samples which confirm the existence of heavy metal is greater in heterostructure composites than the pure NGO and iron oxide nanoparticles. The NGO and Fe_3O_4-NGO are disrupted due to the presence of heavy metal and stress/strain of materials. The rupturing of surface and some points on the surface area is more and higher in NGO that Fe_3O_4-NGO is due to that porous nature of NGO and disruption in layered sheet of NGO can be seen in the Fig. S2. A clear vision of extra or foreign materials existence/incorporation on the surface of sample materials can be identified in the image of NGO, Fe_3O_4 and Fe_3O_4-NGO. When compared to pure sample before adsorption test. From SEM image of NGO clearly shows a very distinct large or wide plane graphene sheets but after the adsorption the graphene sheets were covered with extra materials that are recovered through adsorption process can be seen in FigS2. The same trend in structural behavior is observed for pure iron oxide and Fe doped NGO samples before and after the adsorption studies. This clearly indicates a good adsorption/sorption of heterostructure fabricated.. The higher amount of extra material existence can be seen for heterostructure than the pure sample after the adsorption test. This confirms a higher amount of metal recovery from the water is higher in heterostructure composites.

3.4. XPS spectra

X-ray photoelectron spectroscopy (XPS) measurements were performed to investigate the composition, surface analysis and binding energy of the hybrid nanocomposites of Fe_3O_4-NGO samples (0.25@Fe-NGO and 1@Fe-NGO) respectively (Fig. 3). As shown in Fig. 3(a), the XPS survey spectrum of nanocomposites consisting of Fe, C, O, and N respectively. The deconvolution spectra of carbon peak were located at 285.0 eV is assigned to carbon C-C/C=C bonding and the carbon bonding with oxygen-containing groups C-O/C=O and C-OH/C-OOH are located at 286.2 eV with low intensity as shown in Fig. 3b for 0.25@Fe-NGO and 1@Fe-NGO respectively. It can be predicted from the Fig. 3(b), that the intensity of carbon and oxygen-carbon functioning is higher for 0.25@Fe-NGO than the 1@Fe-NGO is due to the presence of higher reduction of GO which involved in the formation of higher amount of magnetite nanoparticles [40]. This indicates a clear reduction of oxygen in NGO and a higher amount of oxygen involved in the formation of magnetite particles. The existence of oxygen can be observed from the Fig. 3(c) and the peaks located at 528.1 eV and 532.5 eV corresponding to O1S spectra for 0.25@Fe-NGO and 1@Fe-NGO respectively. It can be inferred from Fig. 3(c) that the intensity level of oxygen is low and there is a shift to the left in 0.25@Fe-NGO and is due to the

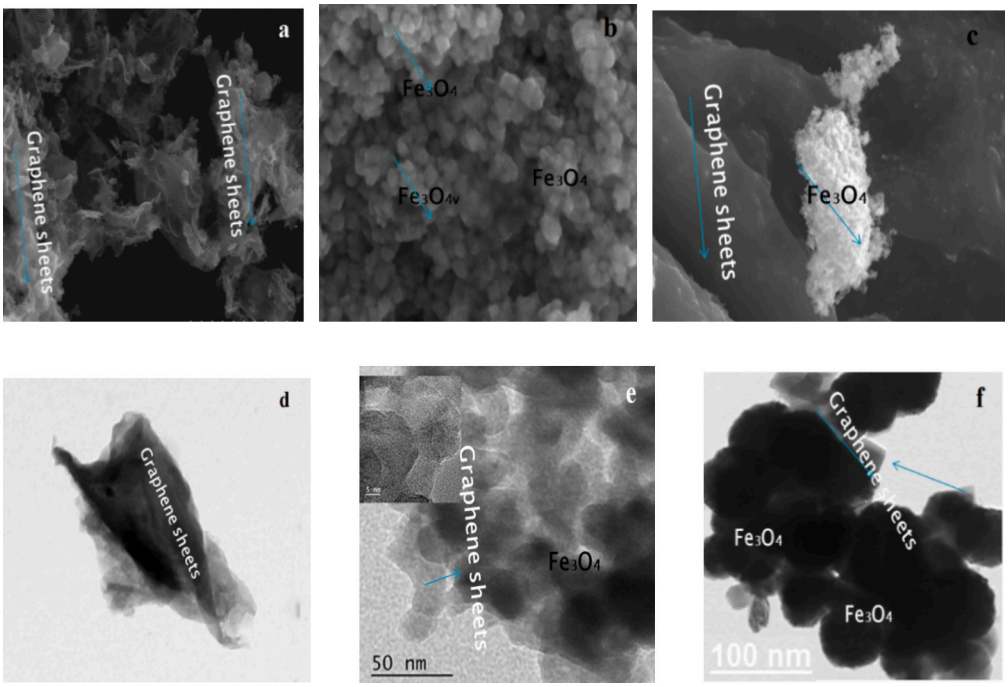

Fig. 2. (a-c) SEM images NGO, Fe_3O_4, and 1@Fe-NGO and (d-f) HR-TEM images of NGO, and 1@Fe-NGO.

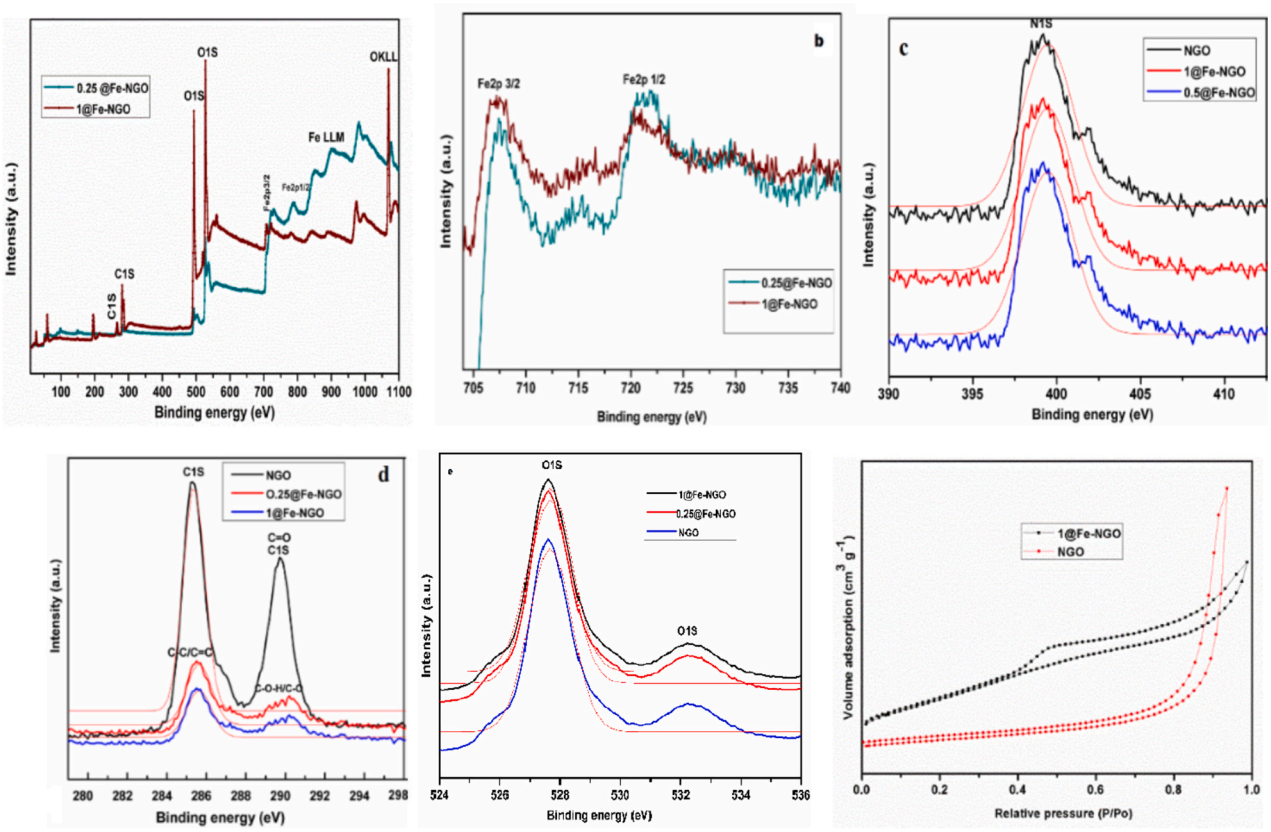

Fig. 3. XPS spectra of (a) survey spectra (b-e) high-resolution spectra of the peak of Fe 3d, N 1S, C1S, and O1S of NGO, 0.25@Fe-NGO and 1@Fe-NGO (f) BET surface area measurement of NGO and 1@Fe-NGO.

oxidation of oxygen in the composite but the intensity level is lower than 1@Fe-NGO due to a higher amount of oxygen participation in magnetite nanoparticles. The estimation of iron in the nanocomposites is predicted from the Fig. 3(d) for 0.25@Fe-NGO and 1@Fe-NGO respectively are located at 709 eV (Fe $2P_{3/2}$) and 724 eV (Fe $2p_{1/2}$). It is observed from the Fig. 3(d), that the intensity level is higher for 1@Fe-NGO than 0.25@Fe-NGO which indicates the higher amount of Fe and O leading to the formation of magnetite particles. From the XPS analysis, it can be predicted that magnetite nanoparticles while decorating on the surface of nitrogen-doped graphene layer shows some disruption caused by the higher rate of potential bonding within the surface area interaction and anti-repulsive oxidation-reduction which lowers the energies. This indicates a left shift in energies inclusive for higher synergism between the Fe_3O_4 and NGO sheets and there is a higher surface plasomic resonance exhibiting an enhanced adsorption/sorption rate which is very essential for adsorptive materials. This coupling of hybrid nanocomposites and chemical composition of binding energies reveal that the materials are supportive of electrocatalyst activity, and high adsorption activity. The XPS spectra of the synthesized materials were tested after the adsorption performance test as shown in Fig. S3. It can be predicted from the survey spectra that there is decrease in peak width and height due to presence of terrestrial heavy metal recovery from effluent. Additionally, we can observe the formation small peaks or humps in the survey spectra due to the presence of heavy metal and there in hybridization or coupling on the surface of layered Fe-NGO sheets. This changes in survey spectra suggest an additionally involvement of heavy metals or recovered mineral which is different from pure spectra of the synthesized materials. In overall, the heterostructure composites shows a excellent and efficient rapid removal of heavy mineral from liquid media and in turn suggest this type of hybrid heterostructure for multipurpose applications. The individual spectra of Pd, Cr, Zn and Cd confirms the adsorption of heavy metals is higher in heterostructure than the pure sample. The intensity and height of the peak is higher for heterostructure than NGO, Fe3O4 samples that confirms a higher amount of metal recovery or existence in composites than that of NGO respectively for Pd, Cr, Zn and Cd can be seen in Fig. S3 (a-d). A very distinct change in individual spectra can be identified when metal incorporated or participated in chemical absorption on the surface of heterostructure composites, the spectra of Pd, Cr, Zn and Cd shows a slight higher shifts to right, that indicates a chemical or physiochemical changes of samples materials and interfacing of foreign materials on the surface of sample and in addition a stress or strain formed on the surface due to coupling of hydroxyl or functional groups on the surface of magnetite based composites is higher than the other samples. In overall observation of XPS after adsorption test reveals a greater or higher participation of heavy metal or recovery by the heterostructure composites,

3.5. *BET surface area measurement*

Volumetric nitrogen adsorption and desorption studies were conducted using Bellsorp mini-II system and the samples were degassed below 1.33 Pa at 90 °C for 1 h and heated up to 350 °C for 6 h (10 °C min^{-1}). The specific surface area was calculated by the BET method in the relative pressure range of 0.04–1.00. BET analysis revealed that the surface area measurement for Fe_3O_4 (80 m^2g^{-1}), NGO (450 m^2g^{-1}) and Fe_3O_4-NGO (364 m^2g^{-1}) as shown in Fig. 3e. The surface area of Fe_3O_4-NGO is higher (4 times larger) than that of Fe_3O_4 indicating that N-GO could more effectively prevent the Fe_3O_4 nanoparticles from agglomeration than NGO, which is inconsistent with the HR-TEM results [16,32]. The BET surface area measurement was conducted for the sample after the adsorption test, the results suggest a decrease in surface area and lower the porosity of the materials that are due to the presence of extra participation of foreign elements. This confirms the presence of heavy metal recovery from the effluent and existence of metal in the

synthesized sample. This material exhibits a high rate of adsorption and recovery rate that can be used for any other kind of recovery shown in Fig. S1b. When compared to pure NGO and Fe_3O_4-NGO sample showed much decrease in surface area and lower porosity and pore volume that suggest the role of Fe incorporation on NGO for better and rapid recovery that well agree with FTIR, XPS results.

3.6. Heavy metal removal from synthetic water

The efficiency of hybrid nanocomposites synthesized was examined for the removal of heavy metals like Cr, Pb, and Ni which were individually mixed thoroughly in water with the respectively adjusted *pH* ($pH = 6.7.8$) were taken for the evaluation. A 20-ppm solution of respective metals were added with 10 mg of catalyst and kept for observation with respect to irradiation time [8,41]. From the UV transmittance spectra, the rate constants values were observed at a regular interval of 30 min respectively and it clearly indicates that the transmittance increases gradually as the time of exposure is extended which in turn confirms the higher reduction of heavy metal or elimination of respective metal ions from the aqueous solution. The concentration of heavy metal removal efficiency for hybrid nanocomposites is better than pure Fe_3O_4 and NGO which concludes that the composites exhibit an excellent and rapid performance for the elimination of metals. An in-depth study of the elimination of metals reveals that the hybrid nanocomposites show 4 folds higher performance than pure Fe_3O_4 and NGO respectively as evident in Fig. 4(a-c) for, Pd, Ni, and Cr. The first order and second order rate reaction for the hybrid nanocomposites were calculated using pseudo reaction. Herein, the photo-elimination reaction obeys the Langmuir Hinshelwood model, follows the first order (pseudo) reaction kinetic given as

$$C_t = C_0 e^{-kt} \text{ and } ln\, C_t/C_0 = -k_t$$

The pseudo first-order kinetic rate of degradation at final irradiation time for 20 ppm are -0.13926, -0.91629, -0.43078, -1.29098, -1.60944, -1.77196 respectively for NGO, 0.25@Fe-NGO, 0.50@Fe-NGO and 1@Fe-NGO.

To understand the robust nature of the materials synthesized, the reusability and stability studies were conducted as shown in Fig. 4 (d) respectively for NGO, Fe_3O_4, 0.25@FeGO and 1@FeGO on Cd, Pd and Cr in the synthetic water in similar conditions with the same pH conditions. From the results, it can be predicted that the removal of heavy metal from the aqueous solution shows a very rigid characteristic of materials without the trailing the physicochemical properties of the synthesized materials. The performance of removal efficiency after 5 cycles reduces by 18 % which is good sign for robust and stable nature of materials and recovery rate is also good compared to first use. Even after 3 cycles use the materials adsorbent capacity reduced to appr, 20 that indicates 80 % of efficient removal of heavy metal by materials. This stability and reusability studies confirms the robust, rigid and concerted nature of material and can further be evaluated. This result shows an excellent synergism and coordination of Fe on NGO sheets.

The synthesized hybrid nanocomposites were further evaluated using the industrial effluent collected from one of the industries in Mysore (Titan valves, Mysore India), a real-time practical application. The effluent water contains the major heavy metals like Zn, Pd, Cd, Cu, Cr, Ni, and Mn. To evaluate the performance of hybrid nanocomposites were treated with the industrial effluent and the removal efficiency of heavy materials with catalyst and without catalyst was analyzed using ICPMS instrumentation method [42]. The results signify that the composites exhibited an excellent elimination of heavy metals from the water and it is better than the pure Fe_3O_4 nanoparticles. The amount of concentration of heavy metal removal compared to pure Fe_3O_4 increased by 3 times and 5 folds of enhancement. As the concentration of iron oxide in the composites increased it is observed that the sorbent nature is further increased and the removal efficiency of heavy metals also increased to a higher level as shown in Fig. 5. Heavy metal removal before and after treating with catalyst has been illustrated in Fig. 5. From Fig. 5, it is evident that the hybrid nanocomposites significantly exhibit an excellent and superior performance in the removal of heavy metals better than the pure Fe_3O_4 nanoparticles. An in-depth study confirms the percentage of removal of heavy metal is 3 times better than the pure Fe_3O_4 and with 97 % of heavy metal removal efficiency was due to excellent synergism. The stability test of the synthesized materials was conducted on the industrial effluent to examine the removal efficiency of composites after 5 cyclic performance can be seen Fig. 5 (c-d). From the cyclic test, it can be predicted that the materials removed almost all the heavy metal shows similar recovery ratio and rapid performance of the first cyclic performance and even after 3 cyclic test, the nanocomposites performance was better and robust but the recovery rate of heavy metal drop by 20 %. The recovery of heavy metal from liquid media was 80 % which is compared to 100 % recovery for the first cycle. This confirms the materials have stable and excellent eliminations of minerals. When compared to pure iron oxide, NGO sheets, the nanocomposites exhibited 5-fold of removal performance even after 5 cyclic performances.

3.7. Effect of pH and catalyst dosage

The effect of pH was investigated for adsorption studies which plays a vital role in heavy metal removal. The adsorbate pH is a crucial variable that influences the electrostatic attraction between the composite and pollutant during adsorption. The heavy metal ions adsorption processes are an essential concept, as most adsorption processes do not exist at low pH values. From our studies, it can be concluded that as the pH value increases the rate of recovery rapidly increases up to pH 6 with nearly 100 % recovery rate for all the heavy metals, after that there is slight decreases in performance of metal removal but the rate of recovery 90 % at pH greater than the 7 as shown in supplementary Fig. S4.

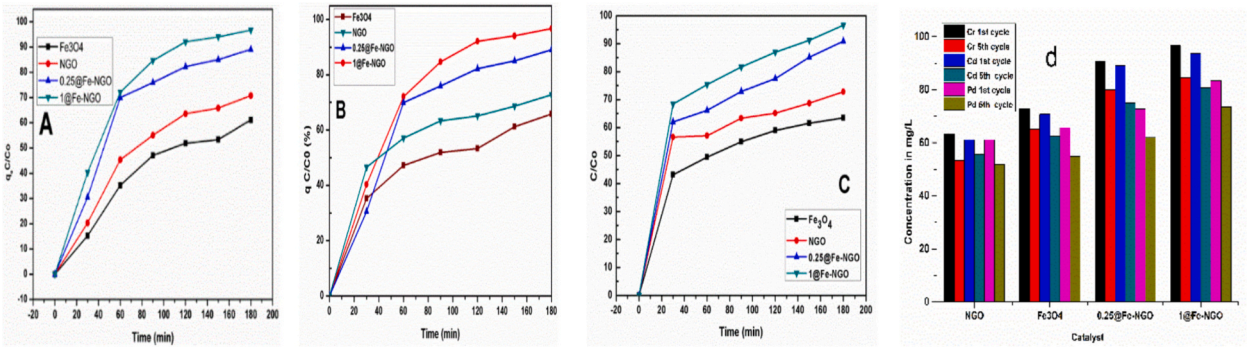

Fig. 4. Removal of heavy metal using NGO, Fe_3O_4, 0.25@FeGO and 1@FeGO respectively for A) Cd, B) Pd, C) Cr) and d) Cd, Pd, Cr removal after 5 cycles (reusability and stability 1 cycle 180 min).

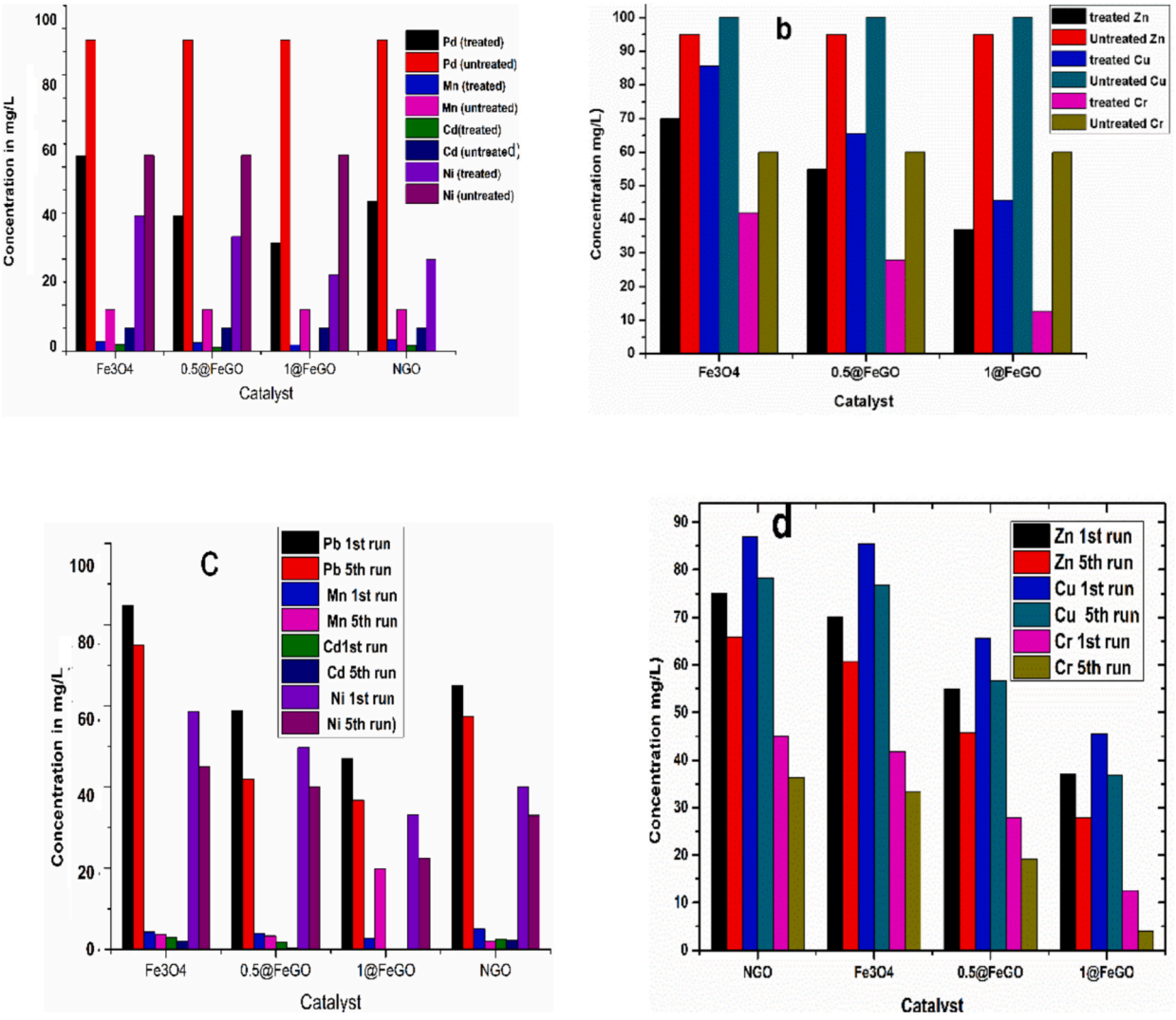

Fig. 5. Sorbent of heavy metals removal from the industrial effiulent befor and after the adsoprtion studies (a c) Pd, Mn, Cd, Ni, and (b-d) Zn, Cu, Cr using the pure Fe_3O_4 and hybrid nanocomposites.

This studies shows a interfacing between adsorbate and adsorption process in endothermic reaction mechanism and showing a good electrostatic and ionic exchange. Additionally, the cata;yst dosage studies were conducted on synthetic water to understand the performance of heterostructure quality and quantitative anlysis on the adsorption performance. A study on gradually increase in catalyst dosage indicates the removal of heavy metal from the water is rapid increases which directly proportional to weight of materials ranging from 5 mg to 20 mg. The performance of metal removal is high as the concentration or dosage of sample is increases but in our studies we employed to use the lower weight percent to understand the feasibility and kinetic behavior can be seen Fig. S4. This indicates that the hybrid nanocomposites showed an excellent coordination and synergism. The result signifies an excellent performance of the hybrid nanocomposites for the removal of heavy metal percentage and its kinetic reaction are given in Table 2. The performance of metal capture and efficiency of metal removal percentage with and without catalyst can be easily understood. The % capture gives a measure of the total analyte removed, the C_k value is a direct measurement of the sorbent affinity for the analyte under the conditions tested. The mass-weighted partition coefficient between the liquid

Table 2
The C_k (solid phase partition coefficient) and % capture of a heavy metal analyst using the sorbent.

Sorbent		Heavy metal analyst						
		Pd	Ni	Cu	Zn	Cr	Cd	Mn
Fe_3O_4	C_k	2700	6000	150,000	15,000	84,000	6000	2600
	% capture	21	37	11	11	46	25	20
NGO	C_k	14,000	15,000	180,000	180,000	28,000	11,000	5300
	% capture	59	60	90	90	78	52	34
0.25@Fe-NGO	C_k	29,000	16,000	200,000	1,200,000	90,000	23,000	10,000
	% capture	80	61	93	97	90	70	51
1@Fe-NGO	C_k	110,000	26,000	260,000	2,400,000	230,000	36,000	60,000
	% capture	97	95	96	100	96	90	90

supernatant phase and the solid sorbent phase and is derived from the equation.

$$\frac{Co - Cf}{Cf} \times \frac{V}{M} = C_k$$

Where C_0 and C_f are the initial and final concentrations of the target analyte in solution (as measured by ICP-MS), V is the volume of the solution in millilitres, and M is the mass of the sorbent in grams.

3.8. Desulfurization

Additionally, the performance of adsorption activity and stability of hybrid composites were further investigated for the removal of sulfur content in thiophene. The adsorption capacities of magnetic Fe_3O_4 nanoparticles on sulfur compounds showed a very low value of 0.475 m molg^{-1} and in case of NGO and Fe_3O_4-NGO, the adsorption capacities are 0.7362 and 1.4750 mmol g^{-1} respectively as shown in Fig. 6A, and have advantages over many other reported adsorbents. Interestingly, when the Fe_3O_4 nanostructures were incorporated in NGO surface, there is an increase in adsorption capacity of N doped GO (Nassar 2010; Hao et al., 2010; Zhang et al., 2010). The adsorption capture tendency of 1@Fe-NGO increased drastically when compared to pure Fe_3O_4 and NGO samples. As the concentration of *ppmw* is increased from 0 to 600, it is observed that the amount of sulfur content adsorbed by the nanocomposites increases which shows a direct interaction. The efficiency and stability performance of desulfurization of the composites were evaluated using time and fixed concentration of *ppmw* as shown in Fig. 6B. At 300 *ppmw* of concentration and with respect to time from 0 min to 400 min was periodically noted at an interval of 60 min as shown in Fig. 6B. As evident from these results, it was observed that the amount of sulfur adsorbed by the composites increases gradually as the time of exposure increases which confirms the stability and durability of the materials for longer run and performance level of the composites also gradually increased. Longer the exposure time the higher sulfur absorption which is a vital material for environmental applications. On the basis of the results, it is obvious that the carbon (GO) and Fe has a good affinity for thiophene and shows excellent synergetic effect. Apart from this synergism, the nitrogen content also plays a vital role in adsorption and its coupling to the composites is due to an extra lone pair of electrons conduction and increase in the surface with a high porosity which acts as capillary action on the surface of the composites. This means that the increase in molecular size of sulfur compounds does not compromise the performance of adsorbents. Fe (III) can form the usual-bonds with the empty *s*-orbitals and, in addition, their *d*-orbitals can back-donate electron density to the antibonding *p*-orbitals (p^*) of the sulfur rings. Finally, it is confirmed that the magnetite nanoparticle decorated on the nitrogen-doped GO hybrid complex hetero-structure can be used for many environment concern and other potential applications.

Fe_3O_4-NGO composites showed excellent adsorption activity for the removal of sulfur and heavy metal from industrial wastewater. The performance is attributed to the higher content of (carbon) graphene and metallic oxide bonding of magnetite nanoparticles encapsulated with the porous nature of NGO sheets and highly active porous sites with a large surface area of NGO.

3.9. Proposed mechanism

The factor responsible for the superior and excellent performance of Fe_3O_4-NGO composites as the absorbent is due to π- π electron overlapping between the adsorbate and the graphene layers and subsequently, the π-electron overlapping of aromatic rings and the graphene layers occurs by π − π or π − σ interaction. The other reason is the electron donor-acceptor mechanism which is mainly initiated by the presence of nitrogen giving an excess lone pair of electrons. This in turn increases the surface area with high porosity, including hydrogen bonding and acid−base interaction which can easily absorb many molecules on the entire surface. Besides this, anchoring of magnetite nanoparticles on the surface of NGO enables to attach/attract the molecules of adsorbent easily because of electronic nature and intrinsic hybridizations of orbitals at different energy bands [43,44].

The sulfur compounds diffuse rapidly and get attracted or attach to the surface of the highly porous nitrogen-doped GO and magnetite nanoparticles followed by entering the pore channels. This acts as a whirlpool sites and higher surface properties having different functional groups and its electronic bonding collectively enhanced the performance. The aromatic sulfur compounds adsorption depends mainly on the (1) interaction of acid-base with adsorbate molecules and metal site or active sites on the surface of adsorbents between NGO and Fe_3O_4, (2) pore structure of metals sites of composites (Fe_3O_4 and NGO) and (3) electron density contribution from the adsorbents because of exposed metal sites and π-π electron interaction which are additionally supported by mesoporous behavior of the composites. In addition, the carbon-oxygen functional groups on the surface of the graphene layer conjugate with heavy metals and sulfur compounds are higher. Even the

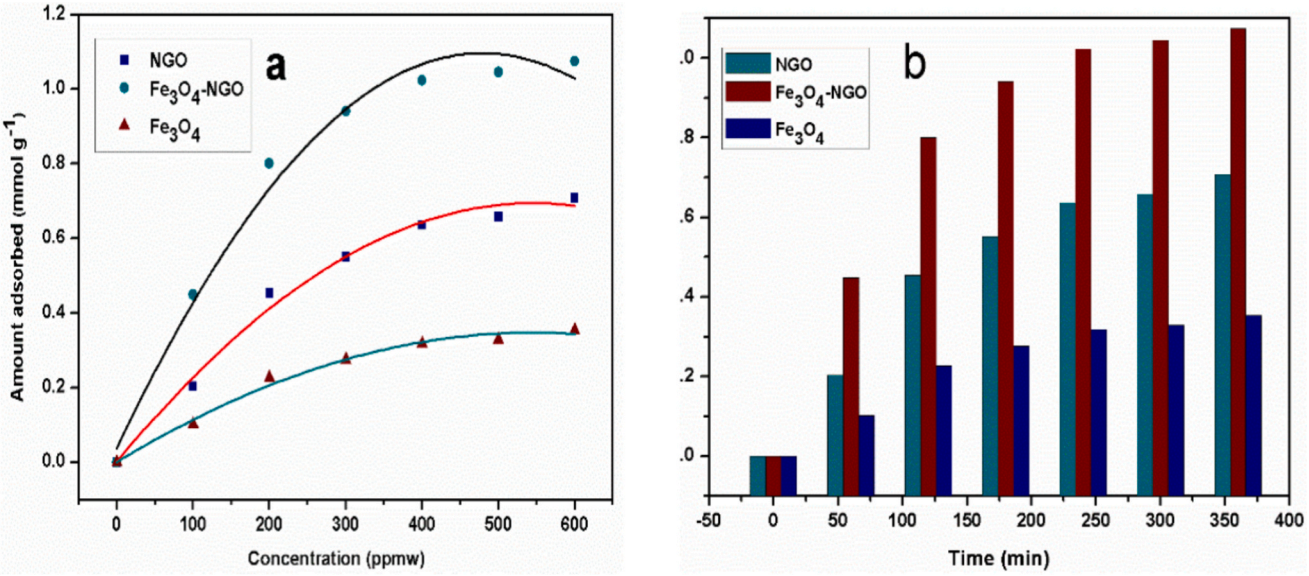

Fig. 6. Adsorption of sulfur a) different *ppmw* levels from 0 to 600; b) stability performance at 300 *ppmw* for Fe_3O_4, NGO, 1@Fe-NGO (Fe_3O_4-NGO composite).

densities of sulfur compounds have different electron nature of bonding which interacted with the nitrogen and GO (carbon-oxygen) and within the Fe_3O_4. The higher adsorption rate is due to higher surface area and porous structure of composite which is better than the pure NGO and Fe_3O_4. This is closer to the molecular size of sulfur compounds and that of the heavy metals which leads to higher potential energy and kinetic rates of reaction. Another factor could be due to the higher porosity of the composites which is very close to the molecular size of thiophene which can easily capture into the surface and interlayer spacing of the composite that eventually increase the absorption. The empathy of GO is already acknowledged as the main factor of a good adsorbent but the use of nitrogen (N) doped GO played a vital role in the adsorption and enhancing the physical properties of the materials. The stability factors can be assigned to the oxygen-containing functional groups of the aromatic matrix. The oxygen-containing functional group tends to bind to the hydrophilic species owing to their electrostatic interactions or hydrogen bonds. Whereas the aromatic matrix is likely to bind to the hydrophobic organics by π-π stacking or hydrophobic interactions and the oxidation level of NGO increases, the adsorption capacity increases. This is due to the extra number of functional groups that were introduced onto the basal plane of GO through the oxidation process, and the increase in the negative charge of the NGO sheets. Furthermore, some of the anionic groups on NGO will be deprotonated at higher *pH* resulting in an enhanced negative charge.

4. Conclusion

The authors have successfully synthesized for the first-time nitrogen-doped layered GO sheets decorated with ultrafine isometric magnetite nanoparticles using sol-gel method followed by microwave treatment. Such a novel approach of hybrid nanostructures fabrication showed an enhanced reaction kinetics with a better performance for the removal of heavy metals in industrial effluent and efficient removal of sulfur. This hybrid composites structure showed an excellent synergism and its coordination improved the physicochemical properties better than the bulk. Rapid removal of heavy metal ions was found to be 5 fold better with over 97 % removal efficiency and the isoprotion of sulfur showed 3 times greater than the pure Fe_3O_4 and NGO sheets is due to the coordination of Fe with carbon doped nitrogen mesoporous composites. This novel advanced functional material can further be used for any potential application in energy and environmental related issues.

Consent for publication

Not applicable.

Ethics approval and consent to participate

Not applicable.

Research involving human and animals rights

Not applicable.

Funding

Not applicable.

CRediT authorship contribution statement

Kashinath Lellala: Writing – original draft, Visualization, Software, Formal analysis, Data curation, Conceptualization. **Subhendu Kumar Behera:** Writing – review & editing, Visualization, Methodology, Investigation, Data curation. **Prarthana Srivastava:** Writing – review & editing, Validation, Investigation, Formal analysis. **Waseem Sharaf Saeed:** Writing – review & editing, Validation, Supervision, Formal analysis. **Ahmed S. Haidyrah:** Writing – review & editing, Validation, Supervision, Investigation, Formal analysis. **Ajay N. Burile:** Writing – review & editing, Writing – original draft, Supervision, Project administration, Methodology, Funding acquisition, Formal analysis, Conceptualization.

Declaration of competing interest

The authors declare that they have no known competing financial interests or personal relationships that could have appeared to influence the work reported in this paper.

Acknowledgments

KL acknowledge Mysore University for experimental facility. The authors are also grateful to the instrument facility of SAIF Kochin, Kerala, India. The authors would like to extend their sincere appreciation to the Researchers Supporting Project number (RSPD2024R755), King Saud University, Riyadh, Saudi Arabia. AB extends gratitude to the Principal of Priyadarshini Bhagwati College of Engineering for the support, encouragement, and facilities provided.

Supplementary data

Supplementary data to this article can be found online at https://doi.org/10.1016/j.diamond.2024.111746.

Data availability

The authors confirm that the data supporting the finding of this study are available within the article. Raw data that support the finding of this investigation are available from the corresponding author, upon reasonable request.

References

[1] Z. Huang, L. Lu, Z. Cai, Z.J. Ren, Individual and competitive removal of heavy metals using capacitive deionization, J. Hazard. Mater. 302 (2016) 323–331, https://doi.org/10.1016/j.jhazmat.2015.09.064.
[2] L. Liu, X. Guo, R. Tallon, X. Huang, J. Chen, Highly porous N-doped graphene nanosheets for rapid removal of heavy metals from water by capacitive deionization, Chem. Commun. 53 (2017) 881–884, https://doi.org/10.1039/C6CC08515F.
[3] X. Gu, Y. Yang, Y. Hu, M. Hu, C. Wang, Fabrication of graphene-based xerogels for removal of heavy metal ions and capacitive deionization, ACS Sustain. Chem. Eng. 3 (2015) 1056–1065, https://doi.org/10.1021/acssuschemeng.5b00193.
[4] T. Humplik, J. Lee, S.C. O'Hern, B.A. Fellman, M.A. Baig, S.F. Hassan, M.A. Atieh, F. Rahman, T. Laoui, R. Karnik, E.N. Wang, Nanostructured materials for water desalination, Nanotechnology 22 (2011) 292001, https://doi.org/10.1088/0957-4484/22/29/292001.
[5] D. Yin, X. Du, H. Liu, Q. Zhang, L. Ma, Facile one-step fabrication of polymer microspheres with high magnetism and armored inorganic particles by Pickering emulsion polymerization, Colloids Surf. A Physicochem. Eng. Asp. 414 (2012) 289–295, https://doi.org/10.1016/j.colsurfa.2012.08.038.
[6] Y. Xue, H. Chen, D. Yu, S. Wang, M. Yardeni, Q. Dai, M. Guo, Y. Liu, F. Lu, J. Qu, L. Dai, Oxidizing metal ions with GO: the in situ formation of magnetic nanoparticles on self-reduced graphene sheets for multifunctional applications, Chem. Commun. 47 (2011) 11689, https://doi.org/10.1039/c1cc14789g.
[7] P. Sharma, M.R. Das, Removal of a cationic dye from aqueous solution using GO nanosheets: investigation of adsorption parameters, J. Chem. Eng. Data 58 (2013) 151–158, https://doi.org/10.1021/je301020n.
[8] H.-Y. Zhu, Y.-Q. Fu, R. Jiang, J.-H. Jiang, L. Xiao, G.-M. Zeng, S.-L. Zhao, Y. Wang, Adsorption removal of congo red onto magnetic cellulose/Fe3O4/activated carbon composite: equilibrium, kinetic and thermodynamic studies, Chem. Eng. J. 173 (2011) 494–502, https://doi.org/10.1016/j.cej.2011.08.020.
[9] C.L. Warner, W. Chouyyok, K.E. Mackie, D. Neiner, L.V. Saraf, T.C. Droubay, M. G. Warner, R.S. Addleman, Manganese doping of magnetic Iron oxide nanoparticles: tailoring surface reactivity for a regenerable heavy metal sorbent, Langmuir 28 (2012) 3931–3937, https://doi.org/10.1021/la2042235.
[10] A.B. Fuertes, P. Tartaj, A facile route for the preparation of superparamagnetic porous carbons, Chem. Mater. 18 (2006) 1675–1679, https://doi.org/10.1021/cm052695e.
[11] X. Guo, B. Du, Q. Wei, J. Yang, L. Hu, L. Yan, W. Xu, Synthesis of amino functionalized magnetic graphenes composite material and its application to remove Cr(VI), Pb(II), Hg(II), Cd(II) and Ni(II) from contaminated water,

J. Hazard. Mater. 278 (2014) 211–220, https://doi.org/10.1016/j.jhazmat.2014.05.075.
[12] H. Wang, T. Maiyalagan, X. Wang, Review on recent progress in nitrogen-doped graphene: synthesis, characterization, and its potential applications, ACS Catal. 2 (2012) 781–794, https://doi.org/10.1021/cs200652y.
[13] J. Su, M. Cao, L. Ren, C. Hu, Fe $_3$ O $_4$ –graphene nanocomposites with improved lithium storage and magnetism properties, J. Phys. Chem. C 115 (2011) 14469–14477, https://doi.org/10.1021/jp201666s.
[14] I.-Y. Jeon, H.-J. Choi, M.J. Ju, I.T. Choi, K. Lim, J. Ko, H.K. Kim, J.C. Kim, J.-J. Lee, D. Shin, S.-M. Jung, J.-M. Seo, M.-J. Kim, N. Park, L. Dai, J.-B. Baek, Direct nitrogen fixation at the edges of graphene nanoplatelets as efficient electrocatalysts for energy conversion, Sci. Rep. 3 (2013) 2260, https://doi.org/10.1038/srep02260.
[15] S. Porada, L. Borchardt, M. Oschatz, M. Bryjak, J.S. Atchison, K.J. Keesman, S. Kaskel, P.M. Biesheuvel, V. Presser, Direct prediction of the desalination performance of porous carbon electrodes for capacitive deionization, Energy Environ. Sci. 6 (2013) 3700, https://doi.org/10.1039/c3ee42209g.
[16] Q. Yuan, N. Li, Y. Chi, W. Geng, W. Yan, Y. Zhao, X. Li, B. Dong, Effect of large pore size of multifunctional mesoporous microsphere on removal of heavy metal ions, J. Hazard. Mater. 254–255 (2013) 157–165, https://doi.org/10.1016/j.jhazmat.2013.03.035.
[17] F.A. AlMarzooqi, A.A. Al Ghaferi, I. Saadat, N. Hilal, Application of capacitive deionisation in water desalination: a review, Desalination 342 (2014) 3–15, https://doi.org/10.1016/j.desal.2014.02.031.
[18] M.E. Suss, S. Porada, X. Sun, P.M. Biesheuvel, J. Yoon, V. Presser, Water desalination via capacitive deionization: what is it and what can we expect from it? Energy Environ. Sci. 8 (2015) 2296–2319, https://doi.org/10.1039/C5EE00519A.
[19] H. Sun, L. Cao, L. Lu, Magnetite/reduced GO nanocomposites: one step solvothermal synthesis and use as a novel platform for removal of dye pollutants, Nano Res. 4 (2011) 550–562, https://doi.org/10.1007/s12274-011-0111-3.
[20] B. Li, H. Cao, J. Yin, Y.A. Wu, J.H. Warner, Synthesis and separation of dyesvia Ni@reduced GO nanostructures, J. Mater. Chem. 22 (2012) 1876–1883, https://doi.org/10.1039/C1JM13032C.
[21] F. He, J. Fan, D. Ma, L. Zhang, C. Leung, H.L. Chan, The attachment of Fe3O4 nanoparticles to GO by covalent bonding, Carbon N Y 48 (2010) 3139–3144, https://doi.org/10.1016/j.carbon.2010.04.052.
[22] Z. Geng, Y. Lin, X. Yu, Q. Shen, L. Ma, Z. Li, N. Pan, X. Wang, Highly efficient dye adsorption and removal: a functional hybrid of reduced GO–Fe3O4 nanoparticles as an easily regenerative adsorbent, J. Mater. Chem. 22 (2012) 3527, https://doi.org/10.1039/c2jm15544c.
[23] L. Wang, R.T. Yang, C. Sun, Graphene and other carbon sorbents for selective adsorption of thiophene from liquid fuel, AICHE J. 59 (2013) 29–32, https://doi.org/10.1002/aic.13896.
[24] H.A. Aziz, Mohd.N. Adlan, K.S. Ariffin, Heavy metals (Cd, Pb, Zn, Ni, Cu and Cr (III)) removal from water in Malaysia: post treatment by high quality limestone, Bioresour. Technol. 99 (2008) 1578–1583, https://doi.org/10.1016/j.biortech.2007.04.007.
[25] H. Ma, X. Qi, Y. Maitani, T. Nagai, Preparation and characterization of superparamagnetic iron oxide nanoparticles stabilized by alginate, Int. J. Pharm. 333 (2007) 177–186, https://doi.org/10.1016/j.ijpharm.2006.10.006.
[26] H. Meng, Z. Zhang, F. Zhao, T. Qiu, J. Yang, Orthogonal optimization design for preparation of Fe3O4 nanoparticles via chemical coprecipitation, Appl. Surf. Sci. 280 (2013) 679–685, https://doi.org/10.1016/j.apsusc.2013.05.041.
[27] M. Almarri, X. Ma, C. Song, Role of surface oxygen-containing functional groups in liquid-phase adsorption of nitrogen compounds on carbon-based adsorbents, Energy Fuel 23 (2009) 3940–3947, https://doi.org/10.1021/ef900051r.
[28] A. Amiri, G. Ahmadi, M. Shanbedi, M. Savari, S.N. Kazi, B.T. Chew, Microwave-assisted synthesis of highly-crumpled, few-layered graphene and nitrogen-doped graphene for use as high-performance electrodes in capacitive deionization, Sci. Rep. 5 (2015) 17503, https://doi.org/10.1038/srep17503.
[29] K. Lellala, K. Namratha, K. Byrappa, Ultrasonication assisted mild solvothermal synthesis and morphology study of few-layered graphene by colloidal suspensions of pristine GO, Microporous Mesoporous Mater. 226 (2016) 522–529, https://doi.org/10.1016/j.micromeso.2016.01.036.
[30] L. Kashinath, K. Namratha, S. Srikantaswamy, A. Vinu, K. Byrappa, Microwave treated sol–gel synthesis and characterization of hybrid ZnS–RGO composites for efficient photodegradation of dyes, New J. Chem. 41 (2017) 1723–1735, https://doi.org/10.1039/C6NJ03716J.
[31] L. Kashinath, K. Namratha, K. Byrappa, Microwave assisted facile hydrothermal synthesis and characterization of zinc oxide flower grown on GO sheets for enhanced photodegradation of dyes, Appl. Surf. Sci. 357 (2015) 1849–1856, https://doi.org/10.1016/j.apsusc.2015.09.072.
[32] K. Lellala, K. Namratha, K. Byrappa, Ultrasonication assisted mild solvothermal synthesis and morphology study of few-layered graphene by colloidal suspensions of pristine GO, Microporous Mesoporous Mater. 226 (2016) 522–529, https://doi.org/10.1016/j.micromeso.2016.01.036.
[33] L. Kashinath, K. Namratha, K. Byrappa, Microwave mediated synthesis and characterization of CeO2-GO hybrid composite for removal of chromium ions and its antibacterial efficiency, J. Environ. Sci. 76 (2019) 65–79, https://doi.org/10.1016/j.jes.2018.03.027.
[34] H. Jabeen, V. Chandra, S. Jung, J.W. Lee, K.S. Kim, S. Bin Kim, Enhanced Cr (vi) removal using iron nanoparticle decorated graphene, Nanoscale 3 (2011) 3583, https://doi.org/10.1039/c1nr10549c.
[35] G. Zhao, X. Ren, X. Gao, X. Tan, J. Li, C. Chen, Y. Huang, X. Wang, Removal of Pb (ii) ions from aqueous solutions on few-layered GO nanosheets, Dalton Trans. 40 (2011) 10945, https://doi.org/10.1039/c1dt11005e.
[36] Y.-M. Hao, C. Man, Z.-B. Hu, Effective removal of Cu (II) ions from aqueous solution by amino-functionalized magnetic nanoparticles, J. Hazard. Mater. 184 (2010) 392–399, https://doi.org/10.1016/j.jhazmat.2010.08.048.
[37] N.N. Nassar, Rapid removal and recovery of Pb(II) from wastewater by magnetic nanoadsorbents, J. Hazard. Mater. 184 (2010) 538–546, https://doi.org/10.1016/j.jhazmat.2010.08.069.
[38] S. Zhang, H. Niu, Y. Cai, X. Zhao, Y. Shi, Arsenite and arsenate adsorption on coprecipitated bimetal oxide magnetic nanomaterials: MnFe2O4 and CoFe2O4, Chem. Eng. J. 158 (2010) 599–607, https://doi.org/10.1016/j.cej.2010.02.013.
[39] S. Dou, A. Shen, L. Tao, S. Wang, Molecular doping of graphene as metal-free electrocatalyst for oxygen reduction reaction, Chem. Commun. 50 (2014) 10672, https://doi.org/10.1039/C4CC05055J.
[40] J. Guo, Q. Zhang, Z. Cai, K. Zhao, Preparation and dye filtration property of electrospun polyhydroxybutyrate–calcium alginate/carbon nanotubes composite nanofibrous filtration membrane, Sep. Purif. Technol. 161 (2016) 69–79, https://doi.org/10.1016/j.seppur.2016.01.036.
[41] Z. Li, C. Xie, J. Wang, A. Meng, F. Zhang, Direct electrochemistry of cholesterol oxidase immobilized on chitosan–graphene and cholesterol sensing, Sensors Actuators B Chem. 208 (2015) 505–511, https://doi.org/10.1016/j.snb.2014.11.054.
[42] P. Shi, N. Ye, Investigation of the adsorption mechanism and preconcentration of sulfonamides using a porphyrin-functionalized Fe 3 O 4 -GO nanocomposite, Talanta 143 (2015) 219–225, https://doi.org/10.1016/j.talanta.2015.05.013.
[43] I.R. Pala, S.L. Brock, ZnS nanoparticle gels for remediation of Pb $^{2+}$ and Hg $^{2+}$ polluted water, ACS Appl. Mater. Interfaces 4 (2012) 2160–2167, https://doi.org/10.1021/am3001538.
[44] U. Chatterjee, S.K. Jewrajka, Amphiphilic poly(acrylonitrile)-co-poly(2-dimethylamino)ethyl methacrylate conetwork-based anion exchange membrane for water desalination, J. Mater. Chem. A Mater. 2 (2014) 8396, https://doi.org/10.1039/c4ta00508b.
[45] L.P. Lingamdinne, H. Roh, Y.-L. Choi, J.R. Koduru, J.-K. Yang, Y.-Y. Chang, Influencing factors on sorption of TNT and RDX using rice husk biochar, J. Ind. Eng. Chem. 32 (2015) 178–186.
[46] L.P. Lingamdinne, Y.-L. Choi, I.-S. Kim, Y.-Y. Chang, J.R. Koduru, J.-K. Yang, Porous graphene oxide based inverse spinel nickel ferrite nanocomposites for the enhanced adsorption removal of arsenic, RSC Adv. 6 (2016) 73776–73789.
[47] L.P. Lingamdinne, J.R. Koduru, Y.-L. Choi, Y.-Y. Chang, J.-K. Yang, Studies onremoval of Pb(II) and Cr(III) using graphene oxide based inverse spinel nickel ferritenano-composite as sorbent, Hydrometallurgy 165 (2016) 64–72.
[48] L.P. Lingamdinne, J.R. Koduru, H. Roh, Y.-L. Choi, Y.-Y. Chang, J.-K. Yang, Adsorption removal of Co(II) from waste-water using graphene oxide, Hydrometallurgy 165 (2016) 90–96.
[49] L. Lingamdinne, I.-S. Kim, J.-H. Ha, Y.-Y. Chang, J. Koduru, J.-K. Yang, Enhanced adsorption removal of Pb(II) and Cr(III) by using nickel ferrite-reduced graphene oxide nanocomposite, Metals 7 (2017) 225.
[50] Kashinath L, Sulphur Embedded On In-Situ Carbon Nanodisc Decorated On Graphene Sheets For Efficient Photocatalytic Activity And Capacitive Deionization Method For Heavy Metal Removal.
[52] Lakshmi Prasanna Lingamdinne, Sreenivasa Kumar Godlaveeti, Ganesh Kumar Reddy Angaru, Yoon-Young Chang, Ramamanohar Reddy Nagireddy, Adinarayana Reddy Somala, Janardhan Reddy Koduru, Highly efficient surface sequestration of Pb2+and Cr3+from water using a Mn3O4 anchored reduced graphene oxide: selective removal of Pb2+from real wate, Chemosphere 299 (2022) 134457.
[53] Lakshmi Prasanna Lingamdinne, Janardhan Reddy Koduru, Rama Rao Karri, A comprehensive review of applications of magnetic graphene oxide-based nanocomposites for sustainable water purification, J. Environ. Manag. 231 (2019) 622–634.
[54] Inamullah Mahara, Faraz Khan Maharb, Nasrullah Mahar, Ayaz Ali Memona, Azhar Ali Ayaz Pirzado, Zeeshan Khatri, Khalid Hussain Thebo, Ayaz Ali, Fabrication and characterization of MXene/carbon composite-based nanofibers (MXene/CNFs) membrane: an efficient adsorbent material for removal of Pb+2 and As+3 ions from water, Chem. Eng. Res. Des. 191 (2023) 462–471.
[56] P. Tan, J.X. Qin, X.Q. Liu, X.Q. Yin, L. Sun, Bin fabrication of magnetically responsive core-shell adsorbents for thiophene capture: AgNO3-functionalized Fe3O4@mesoporous SiO2 microspheres, J. Mater. Chem. A 2 (2014) 4698–4705, https://doi.org/10.1039/c3ta14491g.
[57] H. Qu, J. Deng, D. Peng, T. Wei, H. Zhang, R. Peng, Selective adsorption of Pb2+in the presence of Mg2+ by layer-by-layer self-assembled MnO2/Mxene composite films, Processes 10 (2022) 641.
[58] Q.U. Ain, M.U. Farooq, M.I. Jalees, Application of magnetic graphene oxide for water purification: heavy metals removal and disinfection, J. Water Process Eng. 33 (2020) 101044.
[59] A. Babakhani, M. Sartaj, Removal of cadmium (II) from aqueous solution using tripolyphosphate cross-linked chitosan, J. Environ. Chem. Eng. 8 (2020) 103842.
[60] M. Akram, H.N. Bhatti, M. Iqbal, S. Noreen, S. Sadaf, Biocomposite efficiency for Cr (VI) adsorption: kinetic, equilibrium and thermodynamics studies, J. Environ. Chem. Eng. 5 (2017) 400–411.
[61] M. Azam, S.M. Wabaidur, M.R. Khan, S.I. Al-Resayes, M.S. Islam, Heavy metal ions removal from aqueous solutions by treated ajwa date pits: kinetic, isotherm, and thermodynamic approach, Polymers 14 (2022) 914.
[62] I. Anastopoulos, G.Z. Kyzas, Are the thermodynamic parameters correctly estimated in liquid-phase adsorption phenomena? J. Mol. Liq. 218 (2016) 174–185.